Development of a bench-scale fluidized bed combustor (FBC) for coal and biomas combustion.

Article *in* Nigerian Journal of Technological Research · April 2015

DOI: 10.4314/njtr.v10i1.4

4 authors:

Olubunmi Popoola
Florida International University
17 PUBLICATIONS **38** CITATIONS
SEE PROFILE

Saheed Adio
Obafemi Awolowo University
37 PUBLICATIONS **499** CITATIONS
SEE PROFILE

Adekola Oke
Obafemi Awolowo University
11 PUBLICATIONS **30** CITATIONS
SEE PROFILE

Abraham A Asere
Obafemi Awolowo University
17 PUBLICATIONS **110** CITATIONS
SEE PROFILE

Popoola et al (2015). Development of a bench-scale fluidized bed combustor for coal and biomas combustion. Vol 10 no 1:17-24.

Development of a bench-scale fluidized bed combustor (FBC) for coal and biomas combustion.

Popoola, O. T.,*S. A. Adio, A. O. Oke and A. A. Asere. Department of Mechanical Engineering, Faculty of Engineering, Obafemi Awolowo University, Ile-ife, Nigeria

Abstract

The high technological level of equipment for combustion of fuels, as well as the necessity for rational and efficient use of non-renewable energy resources, has resulted demanding requirements that must be fulfilled by equipment for energy production, via combustion. These requirements form the characteristics of Fluidized bed Combustor (FBC). The objective of this work is to design and fabricate a Circulating FBC for the combustion of coal and biomass and present the design criteria considered in the combustion process. The Designed FBC was then tested by combusting coal (Lafia Obi) and biomass (coconut shell) using the relevant ASTM guidelines. For coal combustion, the characteristic quantities measured from the bench-scale fluidized bed combustion include a mean NO_x emission of 455.35, 376.69, 323.35 and 277.35 ppm for a coal feed size of 10, 15, 20 and 25 mm respectively. NO_x emission from the combustion of coconut shell in fluidized bed is low and further reduced by the introduction of secondary air. Secondary air increases the recoverable energy level from this biomass, while average CO emission was 13,080 16,620 17,040 and 19,140 ppm for a coal feed size of 10, 15, 20 and 25mm. The temperature in the fluidized bed at $\geq 1100^oC$ was sustained.

Keywords: Combustion emissions; fluidized-bed combustion; Design; Lafia-Obi Coal Biomass; Temperature.

Email: *otpopoola@oauife.edu.ng
Received: 2014/06/26
Accepted: 2015/03/20
DOI: http://dx.doi.org/10.4314/njtr.v10i1.4

Introduction

Technological advancements of equipments needed for combustion of liquid and gaseous fuels, as well as the rational and efficient use of non-renewable energy resources, has resulted in requirements that must be fulfilled by equipment for energy production, via coal combustion (Harrington 1985; Manaker 1985; Vangham 1985; Oka 2004). These requirements which form the characteristics of FBC may be summarized as follows; combust low-grade coals with high content of moisture (up to 60%), ash (up to 70%) and Sulphur (6-10%), effectively and inexpensively; effectively combust miscellaneous waste fuels, biomass and industrial and domestic wastes; achieve high combustion efficiency (>99%); achieve boiler flexibility with type and quality of coal; provide effective environmental protection from SO_2, NO_X and solid particles (SO_2 < 400 mg/m^3, $N0_X$< 200 mg/m^3, solid particles < 50 mg/m^3); achieve a wide range of load turndown ratio (20-100%); and enable automatic start-up and control of operational parameters of the plant.

FBC necessarily consists of some major components which are the riser, fluidization device, air distribution device (air blower and/or compressor), particulate collection device and fuel feeding device (Tavoulareas, 1991). The quality of fluidization is strongly influenced by the type of gas distributor used. The most affordable and available design for the air distribution is the flat single perforated plate type. As a distributor plate is required for uniform and stable fluidization (Oka, 2004) so also a plenum chamber. The major parameters to be determined are the volume of the air plenum, the position and type of entry.

Particle characterization is important in all aspects of particle production, manufacturing, handling, processing, and applications. Characterization of particles includes not only the intrinsic static parameters (such as size, density, shape, and morphology) but also their dynamic behavior in relation to fluid flow (such as drag coefficient and terminal velocity) (Yang 2003). The complete characterization of a single particle requires the measurement and definition of the particle characteristics such as size, density, shape, and surface morphology. Particle properties and shapes play an important role in the fluidization process. Different particle configurations and densities behave hydro-dynamically differently at different pressure drops in the bed; thus the bed experiences different velocities of the gas and particles.

During the course of this project, a number of significant research data has been published using the combustor for a wide variety of experimental investigation (Adio *et. al.* 2009; Popoola and Asere, 2011; Popoola and Asere 2013) using a novel FBC designed in-house for the purpose of the investigation. The focus of this work is to present the design procedure as well as the design considerations incorporated into the combustor with the view of formalizing the FBC into a patent.

Materials and Methods.

Single particle characterization.

Many diameters have been defined to characterize irregular particles. The ones used for this design are as follows.

Volume diameter

The volume diameter, d_V, is defined as the diameter of a sphere having the same volume as the particle and can be expressed mathematically as:

$$d_v = \left(\frac{6V_p}{\pi}\right)^{\frac{1}{3}} \quad (1)$$

V_p is the volume of the particle.

Surface diameter

The surface diameter, d_S, is defined as the diameter of a sphere having the same surface area of the particle. Mathematically it can be shown to be

$$d_s = \left(\frac{S_p}{\pi}\right)^{\frac{1}{2}} \quad (2)$$

S_p is the surface area of the particle.

Sieve diameter

The sieve diameter, *dA*, is defined as the width of the minimum square aperture in the sieve screen through which the particle will pass.

Feret diameter.

The Feret diameter, *dF*, is a statistical diameter representing the mean value of the distances between pairs of parallel tangents to a projected outline of the particle, as shown in Fig. 1. The Feret diameter is usually used in particle characterization employing the optical imaging technique.

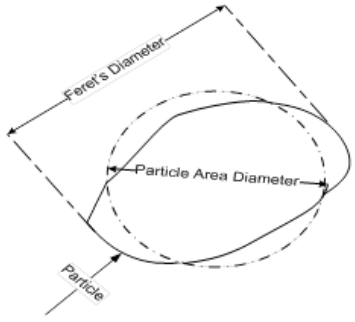

Fig 1: Illustration for projected area diameter, Feret diameter.

Perimeter diameter

The perimeter diameter, d_C, is the diameter of a circle having the same perimeter as the projected outline of the particle.

Surface–Volume Diameter

The surface–volume diameter, d_{SV}, also known as the Sauter diameter, is defined as the diameter of a sphere having the same external-surface-area-to-volume ratio as the particle. This can be expressed as:

$$d_{sv} = \left(\frac{6V_p}{S_p}\right) = \frac{d_v^3}{d_s^2} \quad (3)$$

Particle dynamics

Minimum Fluidization Velocity

Minimum Fluidization Velocity (MFV) is the velocity at which fluidization starts. At this stage, particle velocity becomes zero. MFV determines the lower limit of the operating gas velocity for any fixed particle. Thus it sets the minimum flow rate of the blower for a given pressure drop in the bed. The onset of fluidization occurs when (drag force by upward moving gas) = (weight of particles) Or (pressure drop across bed) *(cross sectional area of tube) = (volume of bed)(fraction of solids) *(specific weight of solids)

$$\Delta P.A_t = (A_t\, L_{mf})\,(1-\epsilon_{mf})((\rho_s-\rho_g)\,{}^{g}/_{g_c}) \quad (4)$$

By re arranging, minimum fluidizing condition gives:

$$\frac{\Delta P}{L_{mf}} = (1-\epsilon_{mf})(\rho_s-\rho_g)\,{}^{g}/_{g_c} \quad (5)$$

In a bed at onset of fluidization, the voidage is a little larger than in a packed bed, and it actually corresponds to the loosest state of a packed bed of hardly any weight. ϵ_{mf} is estimated from random packing data or better still, it could be determined experimentally.

According to Kunii and Levenspiel (1991), the minimum fluidization velocity for a small particle of small specific weight is :

$$u_{mf} = \frac{(\Phi_s d_p)^2}{150}.\frac{\rho_{s-}\rho_g}{\mu}\mathrm{g}\left(\frac{{\epsilon_{mf}}^3}{1-\epsilon_{mf}}\right)$$

{ for $R_e < 20$} (6)

and for large particles

$${u_{mf}}^2 = \frac{(\Phi_s d_p)^2}{1.75}.\frac{\rho_{s-}\rho_g}{\mu}\mathrm{g}{\epsilon_{mf}}^3$$

{for $R_e > 1000$} (7)

If ϵ_{mf} and/or Φ_s are unknown, the following modifications of the expression, suggested by (Wen and Yu 2013) could be employed for a wide variety of systems (Kunii and Levenspiel 1991)).

$$\frac{1}{{\Phi_s\epsilon_{mf}}^3} \cong 14 \;\; and \;\; \frac{1-\epsilon_{mf}}{{\Phi_s}^2{\epsilon_{mf}}^2} \cong 11 \quad (8)$$

Substituting equation (8) into equations (6) and (7) give minimum fluidization velocity for small and large particles respectively

$$u_{mf} = {d_p}^2\frac{(\rho_s-\rho_g)g}{1650\mu} \quad \text{for } R_e < 20 \quad (9)$$

and for large particles

$$u_{mf}{}^2 = d_p{}^2 \frac{(\rho_s - \rho_g)g}{24.5\rho_g} \quad \text{for } R_e > 1000 \qquad (10)$$

These simplified expressions (eqn. (9) and (10)) give U_{mf} in terms of the usually specified variable of densities, particle sizes and gas viscosity; and for 284 data points in a Reynolds number range of 0.001 to 4000 these expressions have been found to give predictions of U_{mf} with a standard deviation of ±34% (Kunii and Levenspiel, 1991).

Terminal Velocity

Terminal settling velocity (TSV) is the velocity reached by a free-falling particle in a stagnant medium. The gas velocity, which is higher than the TSV, will throw the particle out of the bed. Gas flow rate in a fluidized bed is limited on one hand by the U_{mf} and on the other hand by entrainment of solids by the gas. When elutriation occurs, these solids must be recycled or replaced by fresh material to maintain steady-state operations (Kunii and Levenspiel 1991). This upper limit to gas flow rate is approximated by the terminal or free-fall velocity of the particles, which can be estimated from fluid mechanics by:

$$U_t = \left\{\frac{4gd_p(\rho_s - \rho_g)}{3\rho_g C_d}\right\}^{1/2} \qquad (11)$$

Where C_d is experimentally determined drag co-efficient:

$$C_{d\ spherical} = \frac{10}{R_{ep}{}^{\frac{1}{2}}}$$

for $0.4 < R_e < 500$ (12)

Hence :

$$U_{t\ sperical} = \frac{4}{225}\left\{\frac{(\rho_s - \rho_g)^2 g^2}{\rho_g \mu}\right\}^{1/3} d_p \qquad (13)$$

Pinchbeck and Popper 1986 derived an equation to estimate $\frac{u_t}{u_{mf}}$ for spherical particles, considering the total force holding a particle in suspension as a sum of viscous resistance and fluid impact for fine particles with Reynolds number of the particle less than 0.4 as:

$$\frac{U_t}{U_{mf}} = 91.6 \qquad (14)$$

For larger particles with

$$Re_p > 1000, \frac{U_t}{U_{mf}} = 8.72 \qquad (15)$$

Hence, the value of particle density, particle diameter, gas density, gas viscosity, and gas temperature must be known in order to calculate terminal settling and minimum fluidizing velocities. These velocities are different for different boundary conditions. Therefore, to find the velocities for different boundary conditions, there is need to simulate each set of boundary conditions in a numerical model.

Combustor Design.

Fluidized bed combustor necessarily consists of some major components which are the riser, fluidization device, air distribution device (air blower and/or compressor), particulate collection device and fuel feeding device. The designed and fabricated fluidized bed combustor used for this research work alongside with other setup is shown in Figure plate 1.

Riser: The fluidized bed riser was designed and fabricated using available data from the literature as presented in Table 1. Based on these parameters, the minimum fluidization velocity U_{mf} was determined using equation (9), which equals 5.3 cm/s. However, Basu (2006) indicated that the fluidization velocity for the particles less than 450μm (group B) is usually 2 -5 times the minimum fluidization velocity which is to minimize carryover of solids from the bed. For the purpose of this design, the fluidization velocity U_{mf} will be taken as 0.20m/s. The terminal velocity 4.86m/s was easily calculated from the value obtained for U_{mf} using eq. (14) (Pinchbeck and Popper 1986). Calculating the Reynold's number with the terminal velocity gave a result of $R_{e\text{-}14.6}$ showing a good agreement with the earlier assumption (R_e<20) . Kunii and Levenspiel (1991) gave the range of the ratio of the total height of the combustion chamber to height of the bed at minimum fluidization to be between 1.2 and 1.4 i.e.

For the purpose of this design:

$$\frac{H}{H_{mf}} = 1.3 \qquad (17)$$

Table 1: Riser design data

Design Parameter	Material/Value
Bed material	Silica Sand
Diameter of bed material (μm)	350-500
Bed temperature(^{o}C)	600-1200
Static bed height (mm)	100
Bed diameter (mm)	150

Also, based on the expression in Kunii and Levenspiel (1991), the overall height of the combustion chamber can be expressed as:

$$H_{total} = TDH + H \qquad (18)$$

TDH is the transport disengaging height which can be obtained from the correlation in Kunii and Levenspiel (1991). The ratio of TDH to the diameter of the combustor for a fluidizing velocity in the neighborhood of 0.20 m/s is 4 (Kunii and Levenspiel, 1991).

$= \frac{\pi D^2}{4} = \frac{3.142 \times 15^2}{4} = 176.7\text{cm}^2$ $\frac{TDH}{diameter} = 4;\ \frac{TDH}{0.15} = 4;\ TDH = 0.6m$

The maximum expanded height of the bed was assumed to be 0.3m, being twice the static bed diameter, therefore from the equation (18) $H_{total} = 0.6 + 0.3 = 0.9m$

Distributor plate: In designing the distributor plate, pressure drop across the plate was taken to be 10% of the pressure drop across the bed (Kunii and Levenspiel, 1991).

$$\Delta P_{plate} = 0.1 \times (\Delta P_{bed}) \quad (19)$$

And

$$\Delta P_{bed} = L_{mf} \times (1 - \varepsilon_{mf}) \times (\rho_s - \rho_g) \quad (20)$$

Where: L_{mf} = 30cm, ε_{mf} = 0.45∴ $\Delta P_{bed} = 30 \times (1 - 0.45) \times (2.6 - 0.0012) = 42.88cm\ of\ water$

$\Delta P_{plate} = 0.1 \times 42.88 = 4.288cm\ of\ water$

Calculating the Reynolds number for the total flow approaching the plate and selecting the corresponding value for the orifice discharge coefficient C_d =0.62 from the graph of orifice discharge coefficient versus Reynolds number (Kunii and Levenspiel, 1991) gives:

$$R_e = \frac{\rho_g \times U_f \times D_{combustor}}{\mu} = \frac{1.2 \times 0.2 \times 0.15}{1.85 \times 10^{-5}} = 1946 \approx 2000$$

Determining the velocity of fluid through the orifice, measured at the approaching density and temperature using equation (21) and substituting values previously obtained gives:

$$U_{or} = C_d\left(\frac{2g\Delta P_{plate}}{\rho_g}\right)^{0.5} \quad (21)$$

$$U_{or} = 0.62\sqrt[2]{\frac{2 \times 981 \times 4.288}{1.18 \times 10^{-3}}} = 1655.5cm/s = 16.55m/s$$

Determining the number of orifices per unit area of distributor, and finding the corresponding orifice diameter as:

$$U_o = \frac{\pi}{4} \times {d_{or}}^2 \times U_{or} \times N_{or} \quad (22a)$$

$$\therefore \quad \frac{U_o}{U_{or}} = \frac{\pi}{4}{d_{or}}^2 \times N_{or} \quad (22b)$$

(where U_o and N_{or} are the superficial fluid velocity and number of orifices per unit area of distributor).

The fraction of open area, substituting values gives: $\frac{U_o}{U_{or}} = \frac{20}{1655.5} = 0.012 = 1.2\%$

The area of the distributor plate is: $N_{or} = \frac{0.38197}{cm^2} \times 176.7cm^2 = 64.9 \approx 70\ orifices$

Plenum chamber: Typical plenum designs showing various configurations for introducing gas into the plenum were provided by Oka (2004) and a suitable design was selected.

Testing

Samples of Lafia-Obi coal were obtained from natural deposits in Lafia, Obi Local Government of Nassarawa state. The sample were ground and sieved using a set of sieves to obtain the fuel equivalent diameter (FED). Proximate and ultimate analyses of the sample were carried out to determine the carbon, ash, volatile matter, and moisture content of the coal. The calorific value of the coal was determined using a bomb calorimeter, after which the coal was combusted in a fluidized bed.

Thermocouples and 8-channel digital readout meters were employed to measure variations in combustion and freeboard temperature. Different FED of coal were fed, at two different feed rates, into the combustor. The combustion process was quenched at different operating conditions using liquid nitrogen to determine the ash and residue characteristics. The residue recovered from the combustor which includes ash, incompletely combusted coal, fragmented coal particles and bed material was characterized. All data gathered were subjected to appropriate statistical analysis. ASTM international procedures (ASTM International, 2004, 2006, 2007a and b, 2008) were used as guidelines for these investigations.

Secondary air ratio investigation was conducted using coconut shell as the biomass fuel, *t*he effect of secondary air in FBC (air staging) is significant in the reduction of poisonous emissions (Okasha 2007) such as NO, NOx, CO, SO2. Studies on air staging in FBC of coconut shell were also carried out to see the individual and overall effect on the emission characteristics.

Results and Discussion

The fluidized bed combustion chamber shown in plate 1 is shown schematically in Fig 2. It consists of a cylindrical steel column of 15 cm internal diameter and 100 cm in height. The combustor has a gas inlet section, cylindrical reactor body, changeable gas distributor plate,

feeding section for solid fuels and an exhaust to which is fitted a gas analyzer. Table 2 provides a summary of the design parameters for the fluidized bed chamber. A sight glass, 50 mm by 30 mm is provided at the top of the column for visual observation of the combustion process in the reactor.

Coal Combustion

Coal Feed Size and Bed Temperature

As the coal was introduced into the combustor, burning coal particles could be seen on the surface of the bed and there was also evidence of volatile burning. This occurred as the coal split into smaller particles with the evolution of volatile matter. The results are shown in Figure 3. The difference in the effect of particle sizes on bed temperature is however made more visible when the feed rate is increased. As the coal particle size increases, char combustion rate and in consequence, bed temperature decreases. The decrease in reaction temperature with increasing coal feed size in the bed could be attributed to the need for heat required to bring the large volume of volatile released to the temperature of the area. Figure 3 is a summary of the trends. It is represented in bar charts showing that general bed temperature reduces with increasing coal particle size. At the same time the Figure shows that combustion bed temperature increases with coal feed rate.

Coal particle size and CO and NO_x emission

As the coal particle size increases, char combustion rate and in consequence bed temperature decreases and this situation causes higher CO concentration in the flue gases. Figure 4 shows the measured change of CO concentration. There were sharp spikes in the line graphs which represent abrupt concentration changes in the amount of CO in the emission. This effect becomes more pronounced with increasing feed particle sizes. This trend is as a result of repeated char particle fragmentation, at the point of critical porosity. It was generally observed that there is an increase in the level of CO emission measured from the exhaust gas with increased coal particle sizes and a decrease in the level of CO with increasing feed rate. Theoretically, as the bed temperature increases, there is an increase in the rate of char combustion and an increase in the CO oxidation rate; this situation causes lower CO concentration in the flue gases.

The mean bed temperature increases with coal feed rate and reduces with increasing coal particle size. These reasons explain the trend observed during the course of this experiment. The Figures show that there is a reduction in CO with increasing temperature. It was observed that as coal particle sizes increase, the difference in the emission level narrowed i.e. the difference between 10mm and 15mm is higher than the difference between 15mm and 20mm etc. Judging from the height of each of the lines above the x-axis, one can see that the CO concentration increases with increasing coal particle size. Figures 5 shows that the NOx emission decreased with increasing coal particle size.

The two Figures are combined in Figure 10 to give a picture of the effect of coal feed rates. In support of this result, Tullin et al. 1993 reported that NOx formation increased with increasing carbon conversion, which was attributed to a decrease in NOx reduction in the pores of char particles as they shrank. This implies that the NOx concentration decreases with increasing particle size.

Secondary Air and Biomass combustion

As the combustion test was on for the three particle sizes (A, B and C) without the introduction of secondary air, measurement of the emissions at the exhaust of the combustor was keenly monitored with Eclipse EGA4 and KANE 425 flue gas analyzers. Another run of combustion was carried out with the introduction of secondary air above the bed and continuous measurement of the emissions was also observed. Table 3 shows the experimental conditions, of which fuel grain size and the secondary air were selected as the major parameters. The effect of secondary air in FBC (air staging) is significant in the reduction of poisonous emissions such as NO, NOx, CO, SO2. Studies on air staging in FBC of coconut shell were also carried out to see the individual and overall effect on the emission characteristics.

Effect of Secondary Air on Temperature Profile of the Combustor

Figure 6 shows the axial temperature profiles for all the particle sizes combusted in the fluidized bed. After the introduction of the secondary air it was seen that the temperature of the freeboard increases which confirm that the burning of the volatile matter from the coconut shell fully takes place at the freeboard, and highest temperature profile was seen in particle C. This also shows that significant energy will be recovered with the introduction of secondary air at the freeboard during this particle combustion.

Plate 1: Fabricated fluidized bed combustor setup

Table 3: Experimental Conditions

Design parameters	Material/value
Type of fuel/ feed size	Lafia-Obi/(5-25mm), Coconut shell/(3.35-10mm)
Bed material / size (µm)	Sandstone/ 350-500
Bed temperature (^oC)	750-1200
Static bed height (m)	0.1
Fuel feed rate	Coal (0.2 and 0.3(kg/min)) Coconut (4kg/min)
Bed diameter (mm)	150
Fluidization Velocity(l/min)	350-2000
Pressure drop across distributor plate (mmH_2O)	43
Pressure drop across bed (mmH_2O)	428.8
Distributor plate	
No. of holes	311
Diameter of holes (mm)	1.5
Thickness (mm)	4
Air flow rates (l/min) 0,20,25	Primary (350) Secondary(0-25)

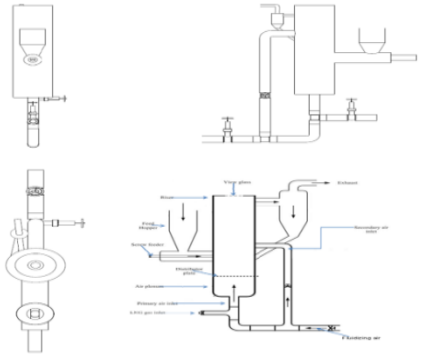

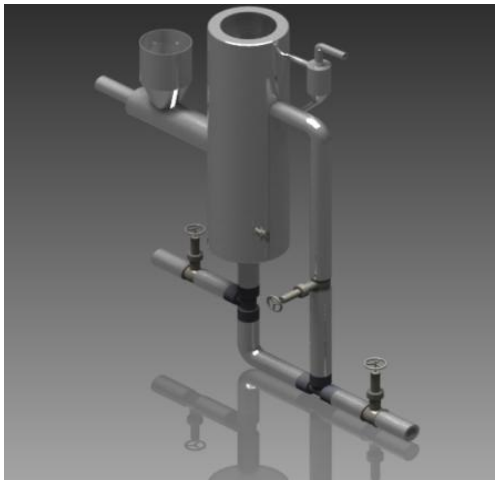

Fig. 2: Schematic diagram of fluidized bed combustion system.

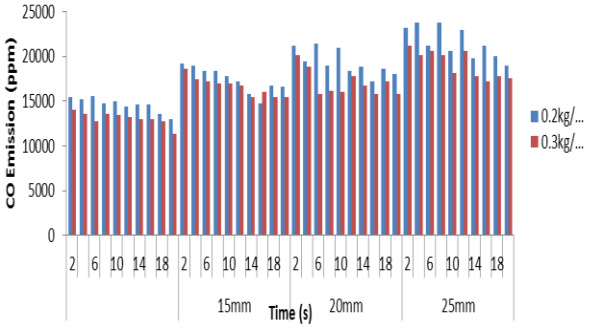

Fig. 3 Summary of the effects of coal particle size and feed rate on temperature

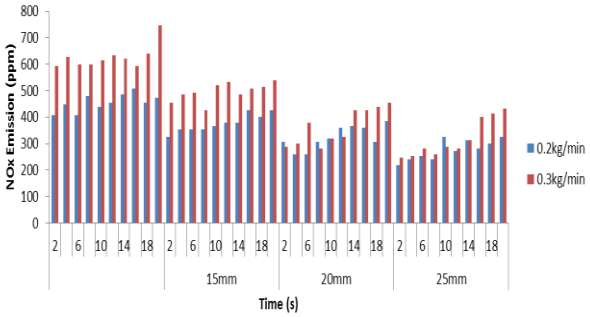

Fig. 4: Summary of the effects of coal particle size and feed rate on CO emission

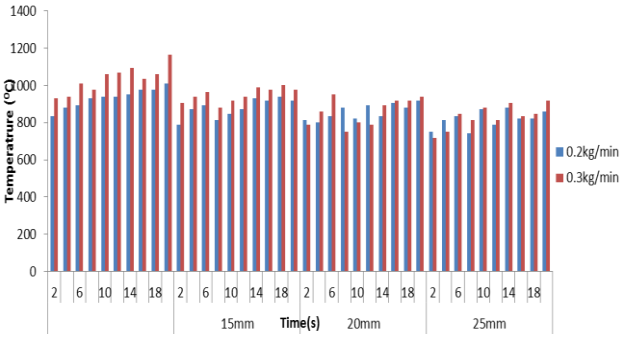

Fig. 5: Summary of the effects of coal particle size and feed rate on NO_X emission.

Secondary Air and CO Emissions

As CO emissions is greatly affected by temperature so also it is affected by the presence of appropriate oxidizing medium (Lyngfelt *et al*, 1998). The overall effect of the secondary air flow rate on CO emissions is given in Fig 7. It can be deduced that there is a great amount of contribution to the reduction of CO when combusting particles A and B, which is not well pronounced in particle C. The results in Fig.7 also show that significant reduction in CO of particles A and B is only noticeable at secondary flow rate of 25 l/min not at any point lower. From this effect on particles A and B, logical hypothesis indicates that at the freeboard, air injection > 25 l/min, reduction in CO emission of particle C will be witnessed. Fig. 8 shows the effect of secondary air with bed temperature on all the particle sizes combusted in the fluidized

bed reactor. The results indicate reduction at various levels of temperature regime in respect of CO.

Effect of Secondary Air on NOx Emission

Reduction in emissions of oxides of Nitrogen has been proven to improve with the introduction of secondary air (Okasha, 2007). In the present study at 20 and 25 l/min secondary air flow rates reductions in the level of NOx emissions were observed. Fig.9 gives the overall behaviour of NOx emission with respect to secondary air emission at different bed temperature.

Table 3 Experimental conditions

Parameters	Values range
Fuel particle types (mm)	3.35-5.00, 5.00-6.30, .30-10
Secondary air flow rates (l/min)	0,20,25
Static bed height (m)	0.10
Fuel feed rate (kg/hr)	4
Primary air flow rate (l/min)	350
Bed material and size (µm)	Silica sand(350-500)
Bed material density (kg/m^3)	2500
Bed temperature (^{o}C)	600-1000

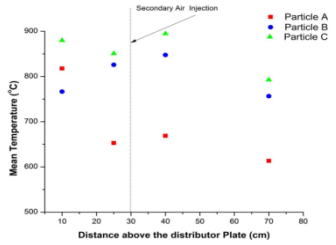

Fig. 6: Axial temperature profiles with secondary air injection Figure

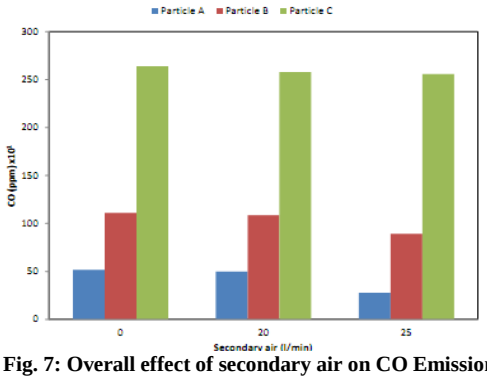

Fig. 7: Overall effect of secondary air on CO Emission

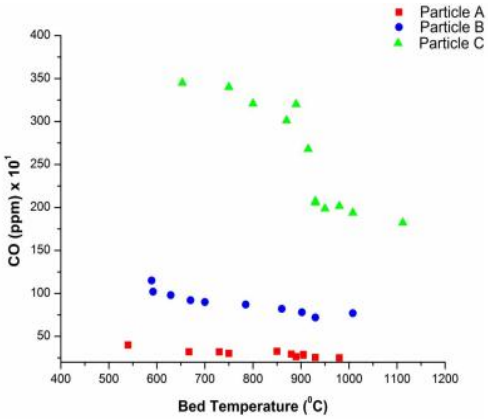

Fig. 8: Effect of secondary air on CO emission at all level of bed temperature

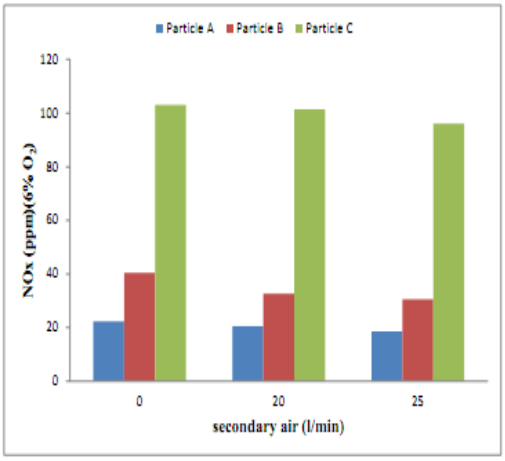

Fig. 9: Overall effects of secondary air on NOx emission of the coconut shell combustion in FBC

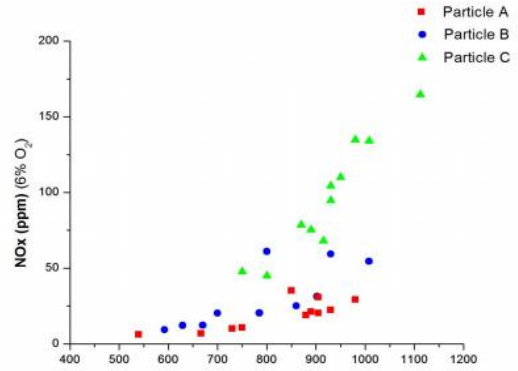

Figure 10: Effect of secondary air on NOx of the coconut shell combustion in FBC

Conclusion

The characteristic quantities measured from the bench-scale fluidized bed combustion during the combustion of Lafia Obi coal include a mean NO_x emission of 455.35, 376.69, 323.35 and 277.35 ppm for a coal feed size of 10, 15, 20 and 25 mm respectively. While average CO emission was 13,080 16,620 17,040 and 19,140 ppm for a coal feed size of 10, 15, 20 and 25mm.

Comparism of the data collected during the testing of the Fluidized bed combustor was in accordance with literature for typical coal combustion. NO_x emission from the combustion of coconut shell in fluidized bed is low and this could be further reduced by the introduction of secondary air. The low emission makes this source of renewable energy environmental friendly. Between the temperatures of 300^{o}C and 650^{o}C of the flue gas, particle B demonstrates lowest level of NOx emission.

Choosing the right size of coconut shell particle the emission of CO and its environmental impact could be reduced to acceptable level. The introduction of secondary air assisted the reduction of the CO emission, as this intensify the post combustion in the freeboard and subsequent overall reduction in the emission

monitored. In the current work particle A gives low level of CO emission. From the temperature in the fluidized bed at $\geq 1100^{o}C$ sustained by the particle, the introduction of secondary air increases the recoverable energy level from this biomass.

References

Adio, S.A.,Odejobi, O. J. , Popoola, O. T. and A. A. Asere. (2009). The potentials of application of fluidized bed combustion in waste to energy generation in Nigeria. In *Proc. of the Annual general meeting of the Nigerian Society of Engineers*. Owerri, pp. 156–162.

ASTM International (2004-2007). *Standard Test Method for Ash in the Analysis Sample of Coal and Coke from Coal.*.

ASTM International, 2008. *Standard Test Method for Moisture in the Analysis Sample of Coal and Coke*

Basu, P. (2006). *Combustion and gasification in fluidized beds*, Taylor & Francis.

Harrington, (1985). A bright new future for coal and fluidized-bed combustion. In *Proc. of the International Conference on FBC*. Houston, pp. 17–24

Kunii, D. and O. Levenspiel (1991). *Fluidization engineering* 2nd ed., Butterworth Heinemann..

Manaker, A.M. (1985). Status of utility fluidized bed commercial development in the United States. In *Proceedings of ASME/IEEE Power Generation Conference*,. Milwaukee, pp. 85–113.

Oka, S. (2004). *Fluidized bed combustion* L.L.Faulkner and E.J.Anthony, eds., Marcel Dekker, Inc.

Okasha, F.,(2007). Staged combustion of rice straw in a fluidized bed. *Experimental Thermal and Fluid Science*. 32:52–59.

Pinchbeck, P.H. and F. Popper (1986). Critical and terminal velocities. *Chemical Engineering Sciences*. 57:78-92.

Popoola, O.T. and A. A. Asere (2013). Emission and Combustion Characteristics of Lafia-Obi Coal in Fluidized Bed Combustor. *Advanced Materials Research*, 824: 318–326.

Popoola, O.T. and A. A. Asere (2011). Investigation of the behaviour of Lafia-Obi coal in a fluidized bed combustor. In *OAUTEKCONF 2011*. Ile ife, pp. 49–51

Tavoulareas, E. S. (1991). Fluidized bed combustion. *Annual Reviews Energy and Environment*. 16:.25–37.

Tullin, C. J., Goel, S., Morhara, A., Sarofim A. F. and J. M. Beer. (1993). NO and N20 Formation for Coal Combustion in a Fluidized Bed : Effect of Carbon Conversion and Bed Temperature. 7: 796–802.

Vangham, W.(1985). Keynote address. Proceedings of 8th International Conference on FBC. In Houston, pp. 1–10

Wen, C. and Y. Yu (2013). Mechanics of fluidization. *Chem. Eng. Prog. Symp. Ser*. 79:.1–12.

Yang, W.-C. (2003). *Handbook of fluidization and fluid-particle systems*, CRC Press.